The Microstructure Design of the Bonding System and Novel Technical Routes for Si_3N_4-Bonded SiC-Refractories

J. Chen, N. Li, Y. Wei, B. Han

In the present work, an overview of Si_3N_4-bonded SiC-refractories, including an optimised bonded system and simplified production process, is given. The so-called Si_3N_4/SiC-bonded SiC-refractories were fabricated via introducing carbon sources into the matrix, with the reaction of carbon and free-Si during nitridation. The results indicated that the optimal nitridation degree and bonded morphology in matrix were achieved in the sample by adding carbon black. They both led to the further improvement in the properties of the final products. Furthermore, from a commercial perspective, there was a considerable impetus to develop low cost methods and simplify the existing technology. So the second objective was to establish a simplified sintering condition and suitable sintering additives for fabricating self-reaction bonded SiC-refractories. Here the alternative sintering atmosphere (in graphite bed) in combination with ferrosilicon was employed. This work was a meaningful attempt with an interesting result. The optimization in the processing and formulation was developed under controlling costs. So it has a potential application and feasibility in the refractory industry.

1 Introduction

There was widespread interest in silicon nitride because of its exceptional elevated temperature properties, including high thermal shock resistance and low creep [1, 2]. An important application area involved adopting direct nitridation of silicon to form in situ Si_3N_4 as bonded phase in SiC-based refractory. Due to the basic chemical nature of Si_3N_4/SiC, Si_3N_4-bonded SiC-refractory possessed excellent properties, e.g. high strength at elevated temperature, low thermal expansion coefficient, high resistance to thermal shock and high corrosion resistance to erosion media and operating conditions, etc. [3–9]. So Si_3N_4-bonded SiC-refractory have played a crucial role in various high-temperature structural applications as non-oxide composite refractories, which are widely used in ironmaking, steelmaking [5, 7] and aluminium making industries [3]. Compared with traditional oxide refractories, the slag corrosion resistance and thermal shock resistance of nitrides bonded refractories have a significant improvement, and many advances benefited the high-temperature industry.

But the incomplete nitriding was a long-standing problem in large-size Si_3N_4/SiC bricks which is associated with the direct nitridation reaction route (RBSN route), and which restricted the further applications. The nitriding depth was approximately 10 mm ~ 12 mm under the existing industrial nitridation route. That nitriding layer which was very dense inhibited nitrogen to penetrate into the inside of the green compacts and further reacted with silicon, so that a casing structure, which was like a box made up of nitriding layer and with SiC and free Si in it, was formed. It led to the heterogeneity of the products, especially for the large-size Si_3N_4-bonded SiC-bricks. The heterogeneity of this structure will degenerate service performance when the refractories materials are used under thermal cycling condition. Because the thermomechanical (expansion coefficients) mismatch among internal and surface layer of Si_3N_4/SiC brick could result in residual stress and, in extreme cases, cracks gradually are generated and propagation and unexpected disastrous spalling during service is at risk (Fig. 1). This kind of defects of final products largely depended on RBSN route.

As a consequence much attention has been given to improving the nitriding degree in the final products. Published literatures have investigated methods like increasing the pressure of nitrogen [10, 11], prolonging nitridation time [11, 12], using finer silicon powder [13] and changing the sintering technology [14]. In addition, many previous studies have shown the positive

Junfeng Chen, Nan Li, Yaowu Wei, Bingqiang Han
The Key State Laboratory of Refractories and Metallurgy
Wuhan University of Science and Technology
Wuhan 430081
China

Corresponding author: *Junfeng Chen*
E-mail: chenjunfengref@163.com

Keywords: Si_3N_4-bonded SiC-refractories, microstructure design, heat-treatment atmosphere, microstructure properties

Received: 15.05.2017
Accepted: 17.10.2017

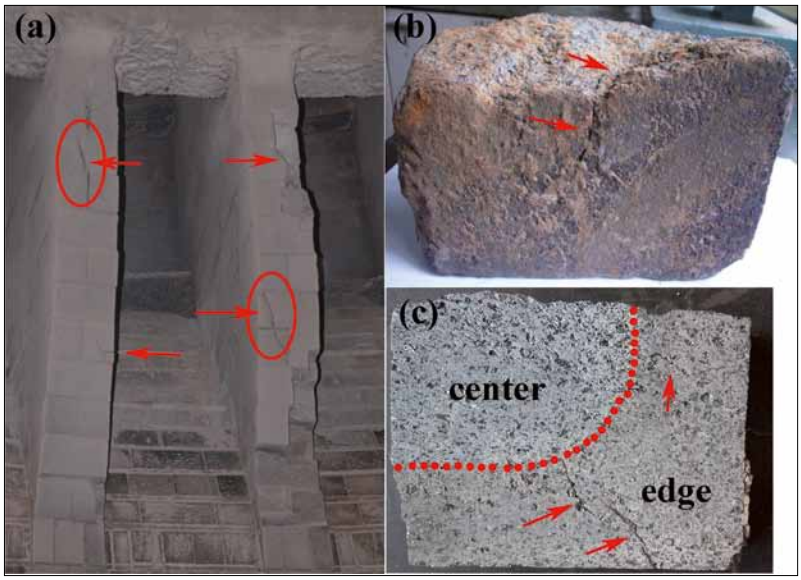

Fig. 1 a–c (a) Si_3N_4-reaction-bonded SiC-bricks applied in ramp area of dry coke quenching furnaces after 18 months; the spalling phenomenon and cracks was found in bricks; (b) cracks were formed in brick edge after 36 months; (c) the cross section morphology of brick shown in (b) [9]

Tab. 1 Experimental formulas of Si_3N_4/SiC refractories system [mass-%]

Ingredient	Composition I			Composition II			
	SNC-re	SNC-g	SNC-cb	NF-0	FS-1	FS-2,5	FS-5
SiC (3~0 mm)	78	78	78	72	72	72	72
Silicon powder	25	23	23	20	19,28	18,20	16,40
Si/G pre-mixed powder	–	+2	–	–	–	–	–
Si/CB pre-mixed powder	–	–	+2	3	3	3	3
Ferrosilicon (in addition)	–	–	–	+0	+1	+2.5	+5
Liquid phenolic resin	+5	+5	+5	5	5	5	5

* Si/X pre-mixed powder refers to that Si and carbon powders pre-mixed in a molar ratio of 1/1, respectively; CB = carbon black; G = graphite

effect of sintering additives, including Y_2O_3 [15], Lu_2O_3 [16], Al_2O_3 [17, 18], ZrO_2 [15, 19], MgO [20] and their mixed additives [14, 18, 19], on the densification, mechanical properties and microstructure of final products. Although considerable efforts have been focused on solving the growing problem, in technology promotion in refractory industry, the progress has been surprisingly slow and there are still huge challenges for the application of large-size Si_3N_4-bonded SiC-brick. It is now time for refractories researchers to consider this issue seriously and take necessary measures to respond to these challenges.

While developing low cost methods and simplifying the existing technology for manufacturing refractories were always desirable and now one of the most challenging research topics in the refractories industry. By considering both above aspects, the present study has a two-fold objective: the initial objective was to design a new bonding system by introducing carbon sources in the matrix, with the expectations that carbon could react with free-Si and be transformed into SiC as secondary bonded phase during nitridation. The reaction between Si and C was independent of N_2; and it has favored the formation of new bonded phase in the sample interior during nitriding process.

And the second work was to fabricate self-reaction silicide/nitride-bonded SiC refractories with a relatively low cost route, by employing simplified sintering conditions (graphite bed) and suitable sintering additives. And the non-oxide ferrosilicon was established as a sintering aid in this work.

2. Experimental

2.1 Preparation process of samples

The compositions of Si_3N_4/SiC refractories samples were shown in Tab. 1. Si_3N_4/SiC refractories were prepared by using commercial grade SiC aggregates (3–1 mm, 1–0 mm, purity ≥98 %, Ruisheng special refractory Co., Ltd. Wuhan/CN), SiC powder (purity ≥98 %, $d_{0,5}$ = 74 µm), silicon powder (purity >98,5 %, $d_{0,5}$ = 27 µm, Wuhan/CN) as main raw materials. Carbon black (purity >99,9 %; Wugang Refractory Co., Ltd./CN) or graphite (purity ≥98 %, $d_{0,5}$ = 74 µm, Zhengzhou, Henan/CN) were used as carbon sources and phenolic resin (36 mass-% of carbon yield, Wuhan/CN) as binder. Ferrosilicon (>97,2 mass-%, $d_{0,5}$ = 1,211 µm, main impurities: 1,44 mass-% Al, 1 mass-% Ca, 0,16 mass-% Mn; Henan/CN) in the ranges 1~5 mass-% were used as additives. The phase analysis and distribution of particle size of ferrosilicon are given in Fig. 2. It was indicated that the main phases of ferrosilicon are silicon and iron silicide. It has to be noted [21] that ferrosilicon was selected as a sintering additive in the bauxite-carbon material system. And it was reported to be very effective in improving mechanical properties, which can be explained with the formation of nano-sized SiC whiskers. Furthermore, ferrosilicon also has cost benefits, compared with rare earth oxides used as sintering additives.

Based on the synthesizing routes, the samples were designated as two main series: SNC-x (nitridation, composition I) and FS-x (reducing atmosphere, composition II), respectively. Furthermore, a series of the nitrided samples were designated as SNC-g (graphite), SNC-cb (carbon black) and SNC-re based on the carbon sources, respectively. The batches of samples also were designated as NF-0, FS-1, FS-2,5 and FS-5 based on the additive contents of ferrosilicon, respectively.

The raw materials with a maximum grain size of 3 mm were mixed in an Eirich intensive mixer (Equipment mode: RO2E, Eirich/DE) with phenolic resin. After kneading, samples with sizes of ∅ 50 mm × 50 mm, 40 mm × 40 mm × 160 mm and 25 mm ×

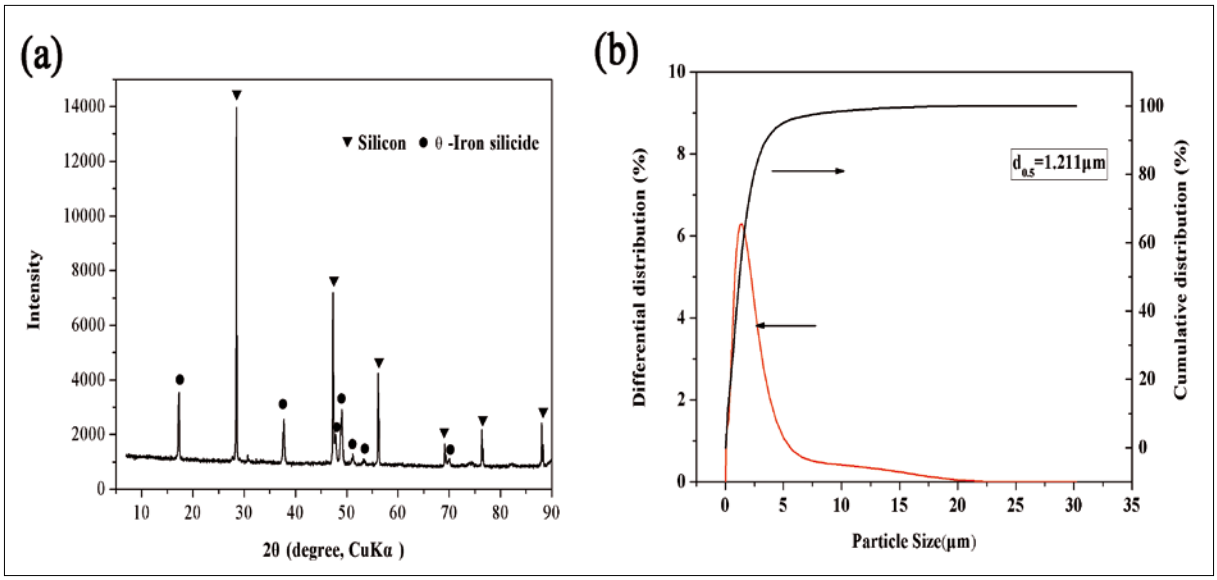

Fig. 2 a–b XRD patterns of ferrosilicon (a), and distribution of particle size of ferrosilicon (b) [22]

30 mm × 140 mm were prepared by cold pressing at 150 MPa and then cured at 220 °C for 24 h.

After that, two processing routes (Fig. 3) were adopted. For the nitrogen treatment, the green compacts were treated in a resistance furnace, under a nitrogen-gas pressure of 0,03 MPa (purity (N_2) >99 %, O_2 impurity). The three-step nitriding sintering was performed by holding the temperature at intermediate 1200 °C for 5 h and 1380 °C for 5 h before heating to the target temperature of 1480 °C for 10 h at a heating rate of 5 K/min (total nitridation schedule = 1200 °C/5 h + 1380 °C/5 h + 1480 °C/10 h). For the second synthesizing route, the samples were placed in a mullite sagger which was filled with graphite powder. Then, the two-step heat treatment was performed in the graphite bed by holding the temperature at intermediate 1200 °C for 3 h before heat to the target temperature of 1450 °C for 6 h was applied at a same heating rate of 5 K/min.

2.2 Testing and characterization methods

After the synthesis, a series of characterization techniques were determined. The phase composition and microstructure were detected by XRD and SEM. For the mechanical behaviour of the fired samples, cold modulus of rupture of sintered samples (40 mm × 40 mm × 160 mm) was measured by three-point bending method with a span of

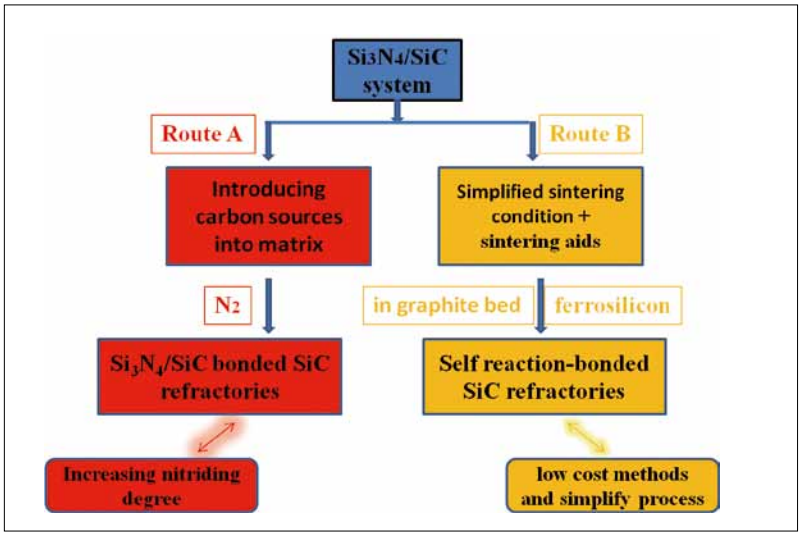

Fig. 3 Schematic of the two processing routes studied here

100 mm. Young's modulus as a function of temperature of samples (140 mm × 30 mm × 25 mm) after heat-treatment was carried out using the concept of the impulse excitation technique (RFDA-HTVP1600, IMCE Ltd./BE). The element content of samples was determined by X-ray fluorescence spectroscopy (XRF, Thermo Scientific ARL 9900 XRF-XRD, Thermo Fisher Scientific Co., Ltd/US). The details of all processing technique in this work are described elsewhere [22, 23].

The main objectives of these tests were to establish the existing corresponding relationships between the technical processing route and final properties, including:

- The microstructure design by introducing carbon resources and nitriding degree of final products;
- Adding ferrosilicon along with changing sintering atmosphere and densification/thermomechanical properties.

3. Results and discussion

3.1 Thermodynamic calculations

The first challenge was to establish the nitridation of silicon and the reaction between silicon and carbon in the co-occurrence under the specific experimental conditions. As a first stage of this strategy, the Gibbs free energy change of eq. (1) and eq. (2)

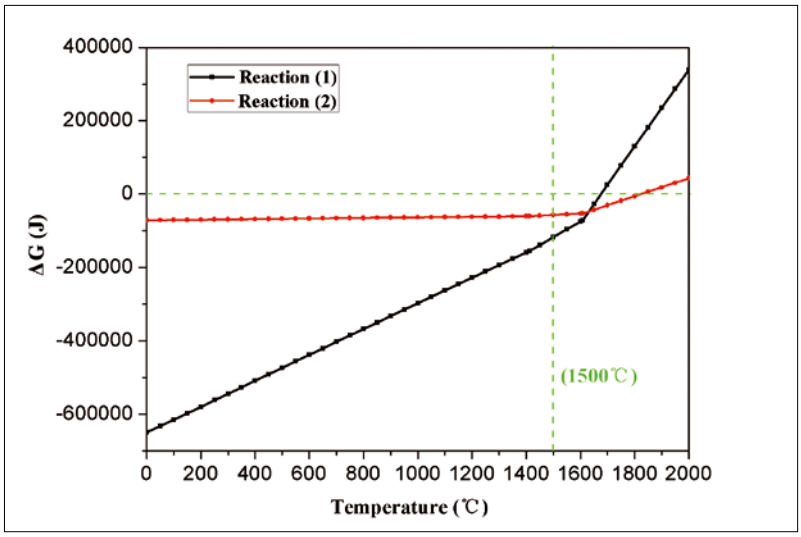

Fig. 4 Changes in Gibbs free energy of reactions (1) and (2) as a function of temperature under 0,03 MPa N_2

was conducted with the version 6.2.0 of the FACTSAGE. The changes in Gibbs free energy of reactions (1) and (2) as a function of temperature under 0,03 MPa N_2 is shown in Fig. 4. The eq. (1) and eq. (2) have large negative ΔG° values below 1873 K. It indicated that the reactions (1) and (2) were favourable below 1873 K. According to the above thermodynamic calculation results, the formation of SiC in the nitridation condition selected are also feasible in theory.

$$3\,Si\,(s, l) + 2N_2(g) \rightarrow Si_3N_4(s) \quad (1)$$

$$Si\,(s, l, g) + C(s) \rightarrow SiC(s) \quad (2)$$

Furthermore, the predominance area diagrams of Si–C–N–O system at soaking temperature (1380 °C and 1480 °C) were also conducted with DOS version 6.2 of FACESAGE (Fig. 5). In the experimental condition, the nitrogen pressure in the furnace was 0,03 MPa, so the $\log_{10}(P(N_2))$ [atm] = – 1,52. In combination with the Si–C–N–O predominance area diagrams, the final reaction product phases were located in the coexisted region of SiC and Si_3N_4. The theoretical analysis proved that SiC and Si_3N_4 both coexisted at 1380 °C and 1480 °C under given condition, when the partial pressures of O_2 in the system was sufficiently low.

Based on above results, the idea was feasible and effective that some silicon carbide compounds can be formed in the matrix of final products after adding carbon during nitridation sintering besides silicon nitride.

In Si–C–N–O system, silicon monoxide and carbon monoxide act as intermediates in the formation of both SiC and Si_3N_4, making their production a competitive process. Therefore, the experimental conditions were of particular importance in establishing which compound will be formed.

3.2 Si_3N_4/SiC-bonded SiC-refractories with difference carbon sources

3.2.1 Influence of carbon sources on the microstructure and nitriding degree of final products

The in situ formed SiC was detected in the final sample with carbon black (Fig. 6 a). To better prove the presence of both Si_3N_4 whiskers and SiC whiskers in the carbon-containing samples, two kinds of whiskers with difference micro-morphology were observed in the same micro region (Fig. 6 b). EDS conformed that the significant differences in element composition between two kinds of whiskers.

The whiskers process bigger in diameter were conformed as Si_3N_4 whiskers, the latter was conformed as SiC whiskers. Additionally, it can be seen that the Si_3N_4 whiskers possess bigger diameter than the SiC whiskers. According to the previous thermodynamic calculation results, the formation of SiC in the experiment condition was also feasible in theory. So based on above results, it was assumed that is feasible and effective to form some silicon carbide compounds in the matrix of final products after adding carbon during nitridation sintering, besides silicon nitride.

According to a sensitive N-element analysis-X-ray fluorescence spectroscopy based

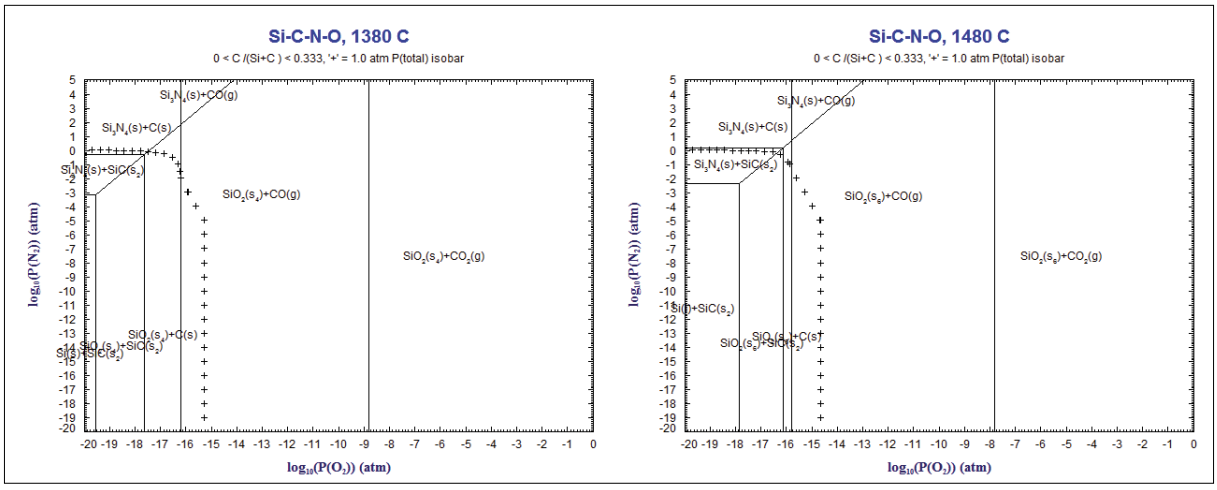

Fig. 5 Si–C–N–O predominance area diagrams at 1380 °C and 1480 °C

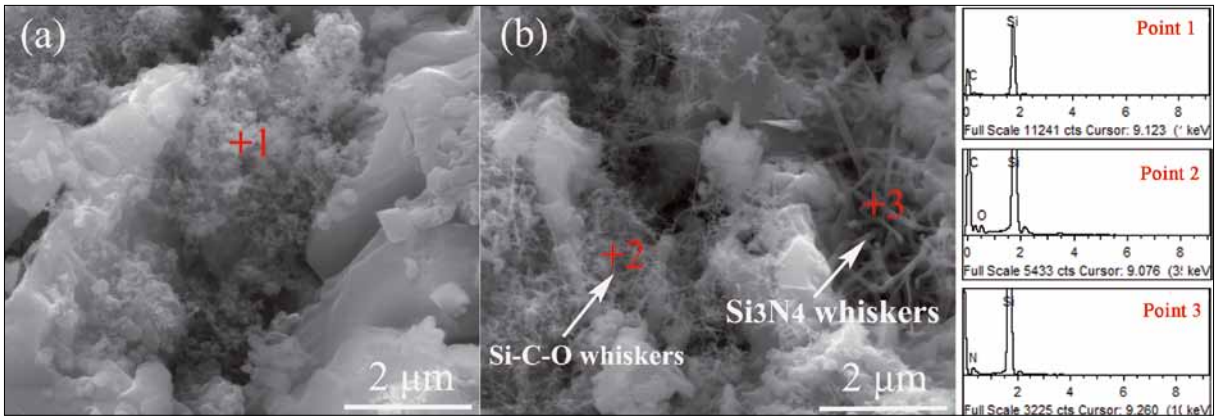

Fig. 6 a–b Si–C–O whiskers and nano-granules formed in sample SNC-cb matrix (SEI): a) SiC nano-granules in sample matrix, and b) Si_3N_4 and SiC whiskers in sample interior (SEI) [23]

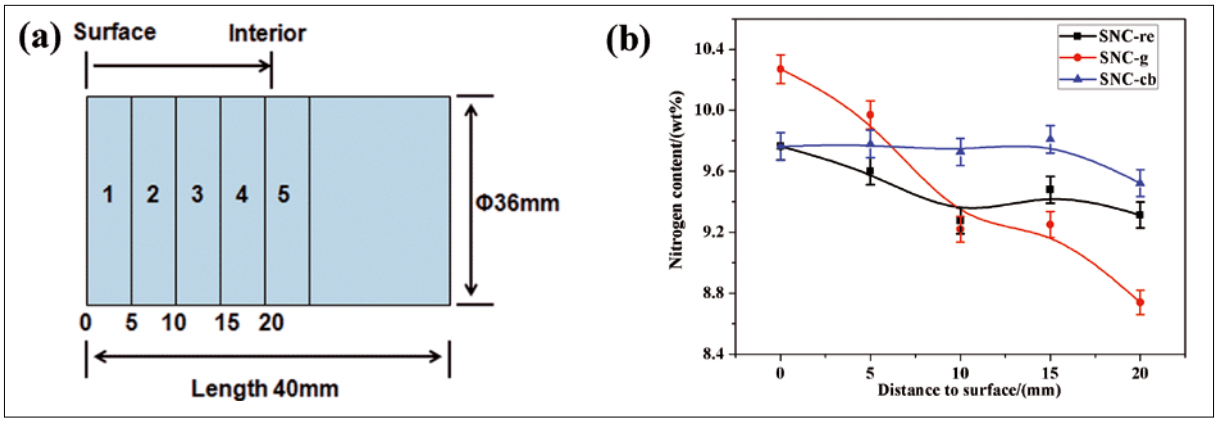

Fig. 7 a–b Schematic diagram of the testing wafers prepared for nitrogen content analysis (a), and the contents of nitrogen as a function of nitriding depth (from sample surface to interior) by using XRF analyser (b) [23]

analytical method, the nitridation degree in different reaction layers of nitriding refractories was also detected. The result is shown in Fig. 7.

What was beyond expectation that the adding of carbon did not only drastically change the bonded microstructure and enhance the mechanical behaviour, but also helped to improve the nitriding process and nitriding degree of the final products. The mechanism to explain the nitriding process is suggested in detail as follow: owing to the micro-pores formed with dispersive distribution through reaction between Si and O a N_2 path into refractory interior is there, which contributing to the permeation of N_2 gas and nitridation of silicon.

The nitrogen content in the sample with carbon black (from sample surface to interior) was overall higher than that of comparative samples. The result indicated that adding carbon black in sample matrix could render Si_3N_4-bonded SiC-refractories homogeneous and optimise the bonded microstructure.

In the case of the sample with graphite, the residual graphite was observed in the sample interior (Fig. 8). The residual graphite maintained its original contour existing between the SiC aggregate and the matrix. A dense SiC_xO_y layer formed on the graphite surface was revealed under a higher magnification. The mechanism of SiCxOy formation

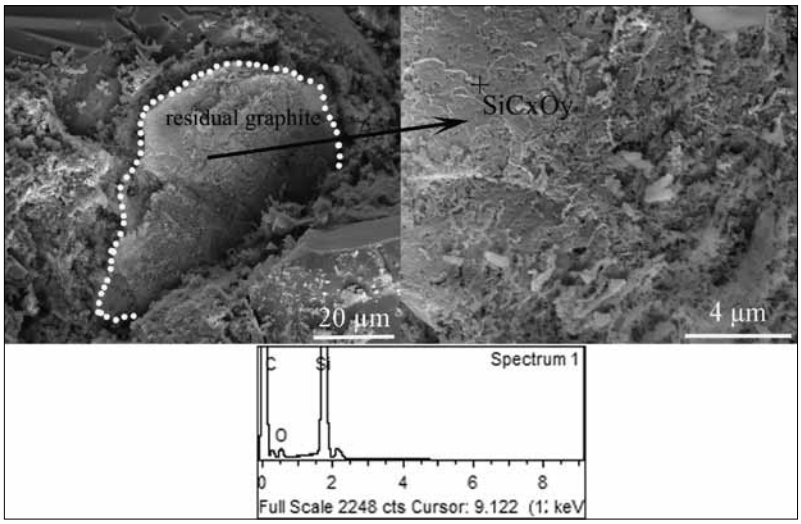

Fig. 8 a–b The bonded morphology in sample SCN-g interior: a) residual graphite existed between SiC aggregate and matrix, and b) SiC_xO_y formed on the residual graphite surface (SEI) [23]

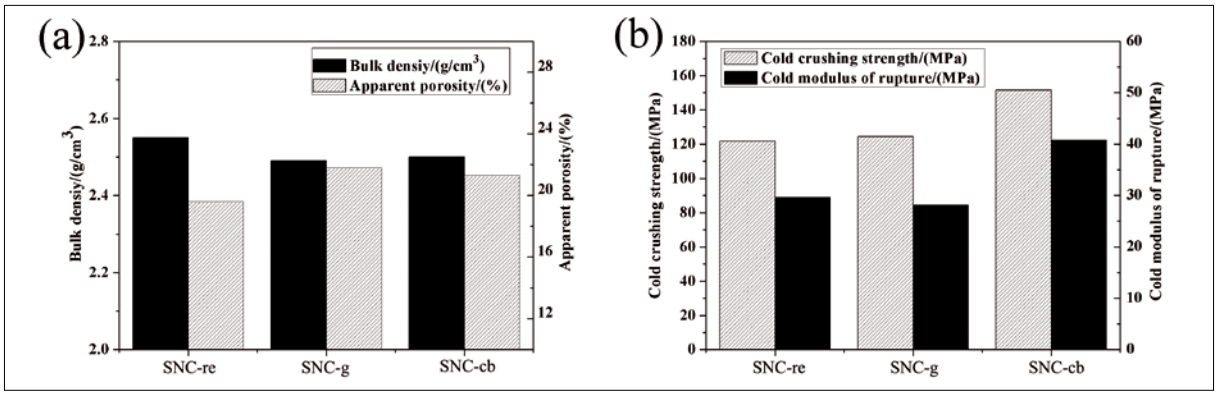

Fig. 9 a–b Force-displacement curves of samples after nitriding treatment

could be described via the liquid (Si)-solid(C) diffusion reaction using graphite as template. The flaky residual graphite remained deteriorated the bonding strength between the SiC aggregate and the matrix, which caused that the mechanical properties were adversely affected. The difference in bonded microstructure and nitridation degree led to the varied in mechanical properties (Fig. 9). The sample with carbon black, CMOR and Young's modulus reached the maximum value of 39,4 MPa and 103,89 GPa respectively, which correspond to 32 % and 41 % improvement of comparative sample.

3.2.2 Influence of carbon sources on the thermomechanical properties of final products

The graphite addition led to a negative effect on the nitridation and strength behaviour of final products. But the behaviour of thermal shock showed an interesting re-

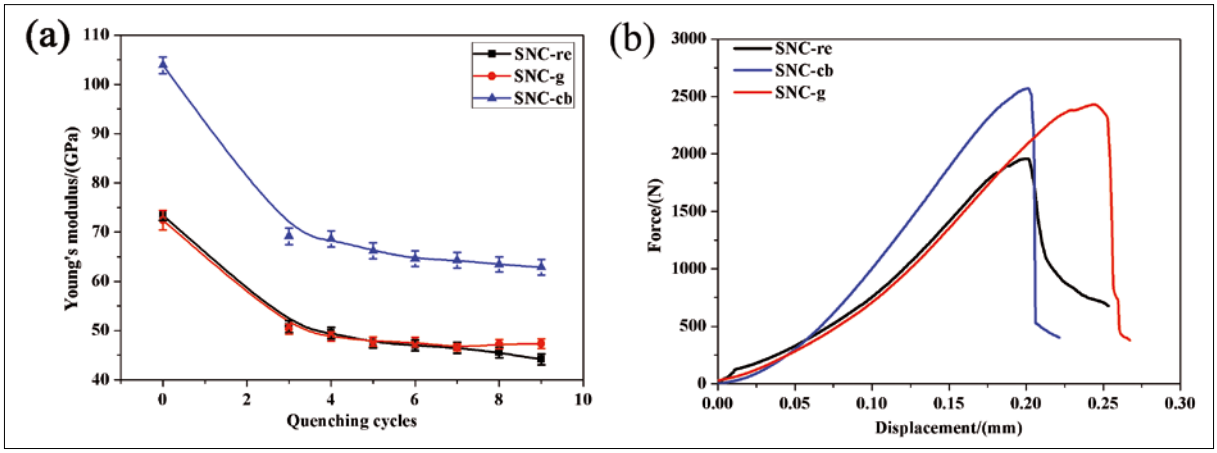

Fig. 10 a–b Evolution of Young's modulus as a function of quenching cycle (samples tested with 1100–20 °C) (a), and force-displacement curves of samples after 9 quenching cycles with samples sizes of 25 mm × 30 mm × 140 mm (b) [23]

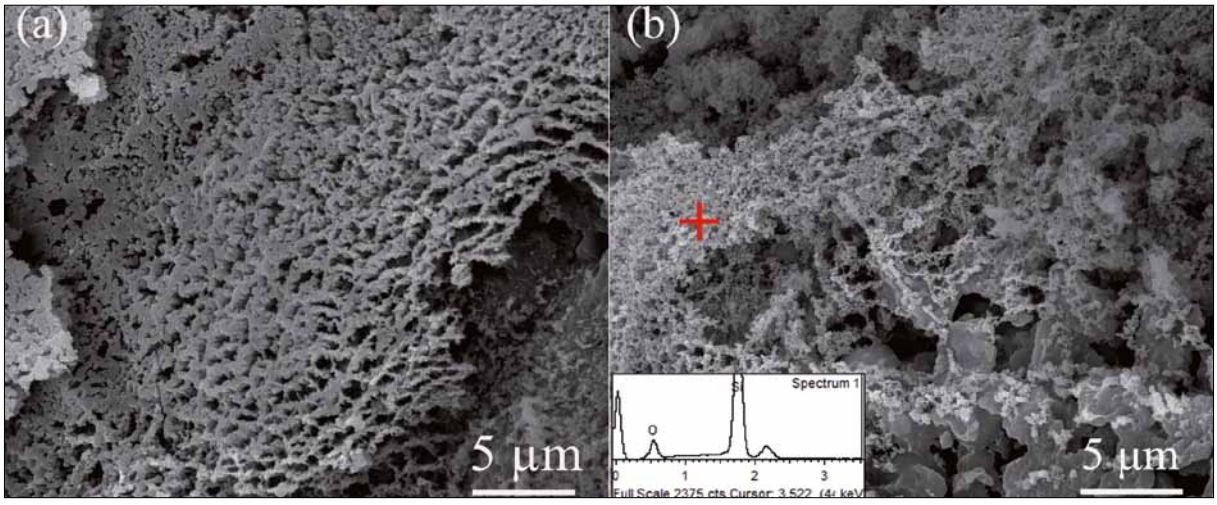

Fig. 11 a–b SEM photograph showing the further reaction occurs in residual graphite in sample SNC-g after 9 quenching cycles

sult (Fig. 10). After 9 quenching cycles, the negative effect of residual flaky graphite on bonding strength was no longer existing in the sample with graphite. The further oxidation reaction of residual graphite led to formation of finer SiO_2 particles, which became a new reinforced phase. This evolution of microstructure of residual graphite can be attributed to the improvement of thermal shock resistance and residual strength. So compared to the carbon black-containing sample with more excellent properties, using graphite to enhance the performance of Si_3N_4–SiC refractory was still a meaningful attempt with an interesting result.

Furthermore, the thermal expansion was an effective prediction index for evaluating refractories service performance. The Si_3N_4/SiC refractories with lower thermal expansion (sample SNC-cb) could improve the service performance effectively (Fig. 12).

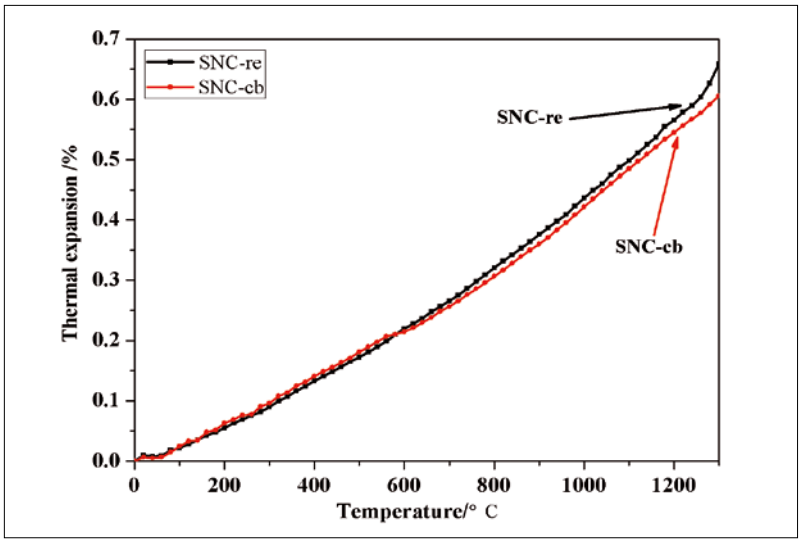

Fig. 12 The thermal expansion of samples as a function of temperature from 20–1300 °C [23]

3.3 The preparation of self-reaction bonded SiC refractories

3.3.1 Elucidating the role ferrosilicon additives on the self-reaction bonded SiC refractories

Tab. 2 presented the phase evolution based on the XRD result of composition II. It has to be noted that α-Si_3N_4 is only be identified in the case of samples with ferrosilicon. The result indicated ferrosilicon could contribute to the formation of α-Si_3N_4. Fig. 13 shows the SiC whiskers and plate-like Si_2N_2O formed in the matrix of samples FS-2.5. It indicates that the nitrides and carbide could be formed after fired in graphite bed.

The further investigation by SEM (Fig. 14) show that the whiskers with tips were formed in the samples with ferrosilicon. Through EDS it is confirmed that they are Si_3N_4 whiskers. Furthermore, EDS analysis of the tip of the whisker confirmed the presence of 17,1 atomic-% Fe along with 82,9 atomic-% Si. The main composition of the whisker was 44,4 atomic-% Si and 55,6 atomic-% N, and confirmed the whisker is Si_3N_4. By considering both the results of XRD and SEM, the formation of Si_3N_4 whiskers with tips was encouraged in the presence of ferrosilicon; which suggested that ferrosilicon had catalytic effects on the formation of Si_3N_4 whiskers via a vapour-liquid-solid (VLS) mechanism. The role of the catalyst could form a liquid solution interface with the crystalline material to be grown and fed from the vapour through the liquid-vapour interface. According to Pavarajarn [24], the liquid phases resulting from the ferrosilicon provided an easy diffusion path for nitrogen to react with silicon, and improved the silicon reacting with nitrogen gas to form α-silicon nitride.

Tab. 3 showed the effect of ferrosilicon additions on the bulk density and apparent porosity of sintered samples. It was observed that the bulk density began to increase gradually up to 2,5 mass-% of ferrosilicon, and finding it increased appreciably, reaching a value of 2,65 g/cm³ at 5 mass-% ferrosilicon. This behaviour can be attributed to the higher true density of ferrosilicon, in comparison to the SiC/Si.

The porosity decreased substantially when the ferrosilicon was added. The weight change rate of samples after firing showed an increasing tendency. The above results confirm that densification was promoted by increasing the amount of ferrosilicon which worked as a sintering aid on the densification. Ferrosilicon also influenced the bond-

Tab. 2 Phase evolution of self-reaction-bonded SiC-refractories after firing in graphite bed

Model Compositions	αα-SiC	α-Si_3N_4	α-Si_3N_4	Silicon Oxynitride	Silicon	Ferrosilicon
NF-0	+	–	+	+	+	–
FS-1	+	+	+	+	+	+
FS-2.5	+	+	+	+	+	+
FS-5	+	+	+	+	+	+

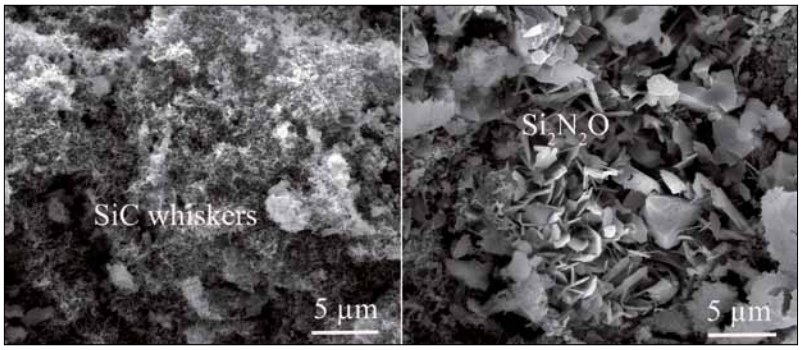

Fig. 13 SEM images of samples matrix, showing that SiC whiskers and plate-like Si_2N_2O formed in the matrix of samples FS-2,5

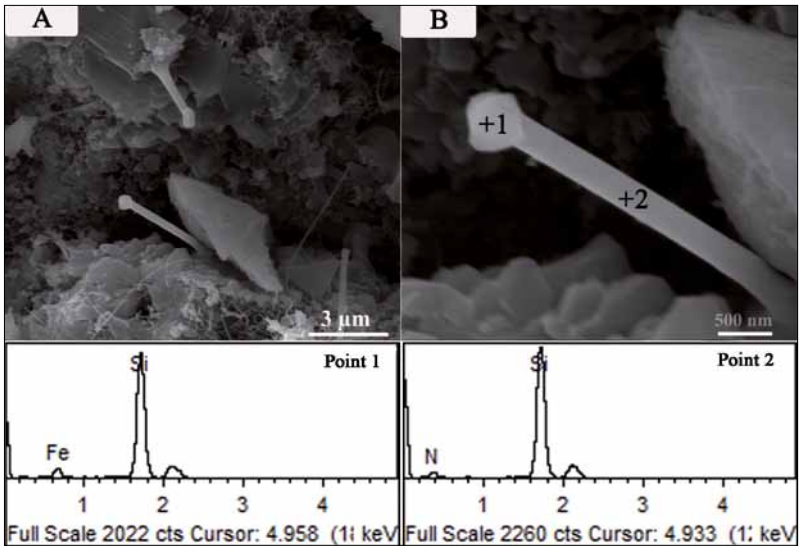

Fig. 14 SEM micrographs of Si_3N_4 whiskers with tips in sample FS-5; B: higher magnification of the Si_3N_4 whiskers in A [22]

Tab. 3 Apparent porosity, bulk density and weight change rate of samples containing different ferrosilicon content after firing

Model Compositions	Apparent Porosity [%]	Bulk Density [g/cm³]	Weight Change Rate [mass-%]
NF-0	18,37	2,42	10,38
FS-1	18,40	2,51	11,80
FS-2.5	17,33	2,52	12,75
FS-5	14,41	2,65	12,84

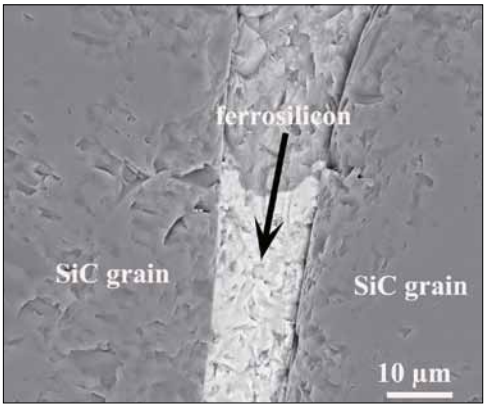

Fig. 15 Backscattered electron image indicates ferrosilicon is present between SiC aggregates of sample FS-5 [22]

ing structure through a direct bonding enhancement (Fig. 15).

In summary, it was identified that the presence of ferrosilicon led to a microstructure development via two main mechanisms. In the first mechanism, ferrosilicon was present between SiC aggregates (Fig. 15). This indicated that the ferrosilicon plays a dominant role in the densification of materials during sintering. In the second mechanism, ferrosilicon was present at the tip of Si_3N_4 fibre, which implied that ferrosilicon has catalytic effects with regard to the formation of the Si_3N_4 fibre.

3.3.2 Interface bonding between SiC aggregate and matrix

Another major factor responsible for the strength properties was the interface microstructure of the SiC aggregate boundaries. It was revealed that a SiCxOy bonded layer exist between SiC aggregate boundary and matrix. Two typical bonded types are: a) the combination of SiC aggregate and matrix via a SiCxOy indirect-bonding layer (left hand in Fig. 16), b) SiC aggregates are directly bonded via a SiCxOy layer (Fig. 16, r.). The formation process of SiCxOy layer in SiC aggregates boundaries is proposed as follows: When the temperature rose to 1450 °C, silicon in the matrix melted and a liquid silicon concentration gradient was formed between the matrix and SiC grain boundary. The liquid silicon had high fluidity and the diffusion of silicon ions through matrix toward SiC grain boundary worked due to the chemical gradient of liquid silicon. The liquid Si can form a firm liquid-

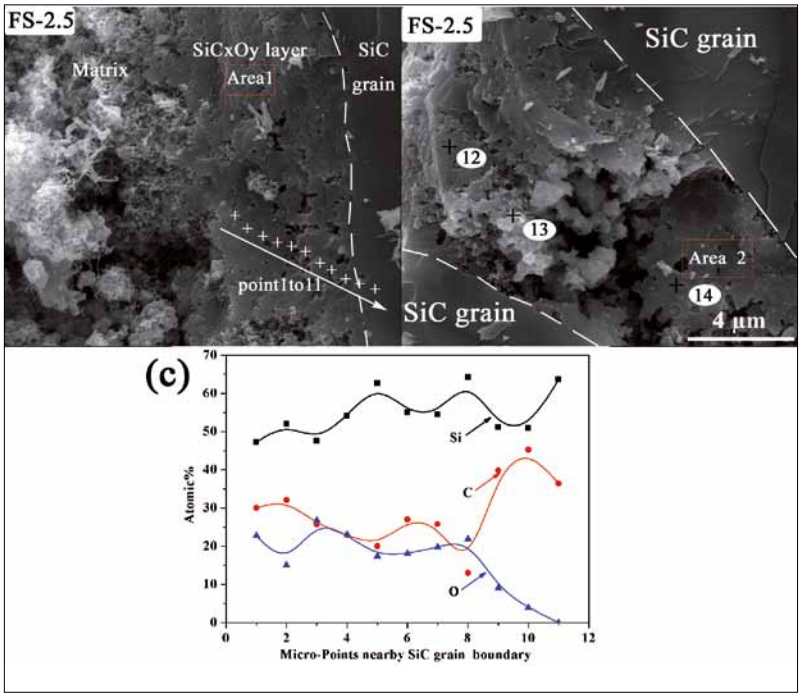

Fig. 16 a–c SEM micrographs of a fracture surface in sample FS2,5, showing the bonded morphology of SiC grain/matrix (a, b); energy spectrum analysis of micro-points nearby SiC grain boundary (c) [22]

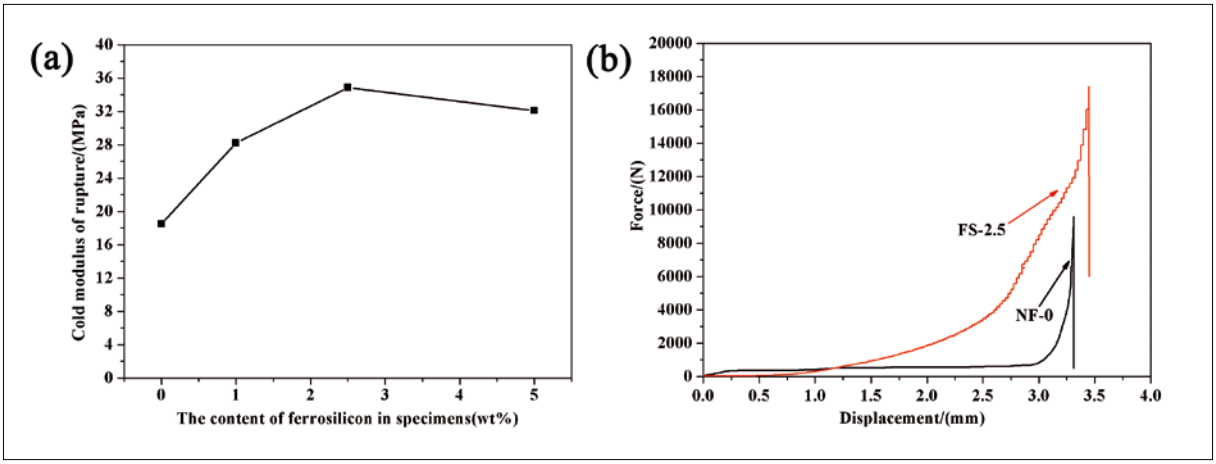

Fig. 17 a–b CMOR of samples containing different ferrosilicon content after firing (a), and force-displacement curves of samples containing 2,5 mass % and without ferrosilicon after firing (b) [22]

solid bonding around the SiC aggregate interface due to the non-reactive wetting of Si on the SiC surface [25, 26]. The surrounding atmospheres in the graphite bed were $3,5 \times 10^4$ Pa CO and $6,5 \times 10^4$ Pa N_2. The CO vapour dissolved into the liquid silicon constantly and SiC_xO_y was formed during the cooling process. The formation of SiC_xO_y was assisted by the solubility of carbon in liquid silicon (e.g. 79 ppm at 1685 K), which was higher than that of nitrogen (e.g. 4 ppm at 1685 K under 0,08 MPa) [27, 28]. It is not difficult to assume that microstructure evolution due to adding of ferrosilicon led to varied properties of final products (as shown in Fig. 17).

The cold modulus of rupture (CMOR) increased with ferrosilicon content up to 2,5 mass-% followed by slight decrease in strength after further increase of the amount of additive. It contributed to the dense texture of the bonded phase and a more refined microstructure. A slight degradation of cold modulus of rupture occurred in sample with 5 mass-% ferrosilicon. This was caused by the formation of an excess liquid phase around inter-granular SiC aggregates boundaries, which created a weak bond.

4 Conclusion

Based on some new research ideas, the development of Si_3N_4/SiC refractories was achieved via different processing routes. From the experimental work, the following conclusion can be made:

- Si_3N_4 bonded SiC refractory reinforced with SiC whiskers/nano-granules were fabricated via introducing carbon. The enhanced nitridation degree was achieved according to this microstructure design when comparing the traditional Si_3N_4 bonded SiC bricks. Thanks to the bonded design of binary-phases, the cold modulus of rupture and Young's modulus of Si_3N_4/SiC-bonded SiC-refractories was enhanced to about 32 % and 41 %, respectively. Furthermore, the homogeneous microstructure resulting from the optimal nitridation degree reduced the thermal mismatch between sample interior and surface. So the thermal shock resistance improved to 42 % after 9 quenching cycles. More importantly, the optimization in the processing and formulation was developed under cost control. It is acceptable for the refractories industry.
- The self-reaction silicide/nitride-bonded SiC refractory was synthesized in a graphite bed and in combination with ferrosilicon. Optimised samples with high densification, strength and Young's modulus were obtained by adding ferrosilicon. The highest strength (34,9 MPa) and Young's modulus of 124 GPa was obtained for a ferrosilicon content of 2,5 mass-%.

Acknowledgments

This work was supported by the National Natural Science Foundation of China (51572203) and 973 Program Earlier Research Project (2014CB660802). The authors would like to thank Wuhan Iron and Steel Group Cooking Co. Ltd. (now China Baowu Steel Group Corporation Limited) for industrially support in this work.

References

[1] Riley, F.L.: Silicon nitride and related materials. J. Amer. Ceram. Soc. **83** (2000) 245–265

[2] Klemm, H.: Silicon nitride for high-temperature applications. J. Amer. Ceram. Soc. **93** (2010) 1501–1522

[3] Wang, Zh.; Skykbakmoen, E.; Grande, T.: Chemical degradation of Si_3N_4-Bonded SiC sidelining materials in aluminium electrolysis cells. J. Amer. Ceram. Soc. **92** (2009) [6] 1296–1302

[4] Changming, K.; Edrees, J.J.; Hendry, A.: Fabrication and microstructure of SiALON-bonded silicon carbide. J. Europ. Ceram. Soc. **19** (1999) [12] 2165–2172

[5] Lee, W.E.; Rainforth, W.M.: Ceramic microstructures, property control by processing. Cambridge 1994, 492–495

[6] Gazulla, M.F.; et al.: Physico-chemical characterisation of silicon carbide refractories. J. Europ. Ceram. Soc. **26** (2006) 3451–3458

[7] Brown, R.W.; et al.: Bond developments in silicon carbide blast furnace refractories during the 1980's, Aachen Proc., 1988, 41–46

[8] Li, X.; et al: Effect of chemical vapour infiltration of SiC on the mechanical and electromagnetic properties of Si_3N_4-SiC ceramic. Scripta Mater. **63** (2010) 657–660

[9] Chen, J.; et al: Synthesis of Si_3N_4/SiC reaction-bonded SiC refractories: the effects of Si/C molar ratio on microstructure and properties. Ceram. Int. **43** (2017) 16518–16524

[10] Priest, H.F.; Priest, G.L.; Gazza, G.E.: Sintering of Si_3N_4 under high nitrogen pressure. J. Amer. Ceram. Soc. **60** (1977) 81–86

[11] Cui, W.; et al.: Effects of nitrogen pressure and diluent content on the morphology of gel-cast-foam-assisted combustion synthesis

of elongated β-Si_3N_4 particles. Ceram. Int. **40** (2014) 12553–12560

[11] Jennings, H.M.: Review on reactions between silicon and nitrogen: Part 1, Mechanisms. J. Mater. Sci. **18** (1983) 951–967

[12] Hu, H.-L.; et al.: Synthesis of porous Si_3N_4/SiC ceramics with rapid nitridation of silicon. J. Europ. Ceram. Soc. **35** (2015) 3781–3787

[13] Liu, Y.D.; Kimura, S.: Fluidized-bed nitridation of fine silicon powder. Powder Technol. **106** (1999) [3] 160–167

[14] Baldacim, S.A.; et al.: Mechanical properties evaluation of hot-pressed Si_3N_4-SiC(w) composites. Int. J. Refract. Met. Hard Mater. **21** (2003) 233–239

[15] Pavarajarn, V.; Kimura, S.: Catalytic effects of metals on direct nitridation of silicon. J. Amer. Ceram. Soc. **84** (2001) 1669–1674

[16] Yang, J.; et al.: Effect of sintering additives on microstructure and mechanical properties of porous silicon nitride ceramics. J. Amer. Ceram. Soc. **89** (2006) [12] 3843–3845

[17] Nourbakhsh, A.A.; Golestani Fard, F.; Rezaie, H.R.: Influence of additives on microstructural changes in nitride bonded SiC refractories. J. Europ. Ceram. Soc. **26** (2006) 1737–1741

[18] Chen, J.; et al.: Effect of Al_2O_3 addition on properties of non-sintered SiC–Si_3N_4 composite refractory materials. Int. J. Refract. Met. Hard Mater. **46** (2014) 6–11

[19] Brahma Raju, G.; et al.: Effect of particle size and oxygen content of Si on processing, microstructure and thermal conductivity of sintered reaction bonded Si_3N_4. J. Alloy. Compd. **595** (2014) 60–66

[20] Strehler, C.; et al.: Influence of sintering and sintering additives on the mechanical and microstructural characteristics of Si_3N_4/SiC wood cutting tools. J. Europ. Ceram. Soc. **30** (2010) 2109–2115

[21] Karamian, E.; et al.: Formation of nano SiC whiskers in bauxite-carbon composite materials and their consequences on strength and density. J. Europ. Ceram. Soc. **31** (2011) 2677–2685

[22] Chen, J.; et al.: Effect of ferrosilicon additive and sintering condition on microstructural evolution and mechanical properties of reaction-bonded SiC refractories. Ceram. Int. **42** (2016) 17650–17658

[23] Chen, J.; et al.: Influence of carbon sources on nitriding process, microstructures and mechanical properties of Si_3N_4 bonded SiC refractories. J. Europ. Ceram. Soc. **37** (2017) 1821–1829

[24] Varong, P.; Shoichi, K.: Catalytic effects of metals on direct nitridation of silicon. J. Amer. Ceram. Soc. **84** (2001) [8] 1669–1674

[25] Woetting, G.; Kanika, B.; Ziegler, G.: Microstructural development microstructural characterization and relation to mechanical properties of dense silicon nitride. In: Int. Conf. on Non-Oxide Technical and Engin. Ceramics, 1985

[26] Liu, G.W; et al.: Survey on wetting of SiC by molten metals. Ceram. Int. **36** (2010) 1177–1188

[27] Yanaba, K.; et al.: Solubility of carbon in liquid silicon equilibrated with silicon carbide. Mater. Transactions. JIM. **38** (1997) [11] 990–994

[28] Narushima, T.; et al.: Nitrogen solubility in liquid silicon. Mater. Transactions. JIM. **35** (1994) [11] 821–826